The Sox Gene *Dichaete* is Expressed in Local Interneurons and Functions in Development of the *Drosophila* Adult Olfactory Circuit

Krishna V. Melnattur,[1,2]* Daniela Berdnik,[3] Zeid Rusan,[1#] Christopher J. Ferreira,[1] John R. Nambu[4]

[1] Biology Department, University of Massachusetts, Amherst, Massachusetts 01003

[2] Program in Molecular and Cell Biology, University of Massachusetts, Amherst, Massachusetts 01003

[3] Department of Biological Sciences, Stanford University, Stanford, California 94305

[4] Department of Biological Sciences, Florida Atlantic University, Boca Raton Florida 33431

ABSTRACT: In insects, the primary sites of integration for olfactory sensory input are the glomeruli in the antennal lobes. Here, axons of olfactory receptor neurons synapse with dendrites of the projection neurons that relay olfactory input to higher brain centers, such as the mushroom bodies and lateral horn. Interactions between olfactory receptor neurons and projection neurons are modulated by excitatory and inhibitory input from a group of local interneurons. While significant insight has been gleaned into the differentiation of olfactory receptor and projection neurons, much less is known about the development and function of the local interneurons. We have found that *Dichaete*, a conserved Sox HMG box gene, is strongly expressed in a cluster of LAAL cells located adjacent to each antennal lobe in the adult brain. Within these clusters, Dichaete protein expression is detected in both cholinergic and GABAergic local interneurons. In contrast, Dichaete expression is not detected in mature or developing projection neurons, or developing olfactory receptor neurons. Analysis of novel viable *Dichaete* mutant alleles revealed misrouting of specific projection neuron dendrites and axons, and alterations in glomeruli organization. These results suggest noncell autonomous functions of Dichaete in projection neuron differentiation as well as a potential role for Dichaete-expressing local interneurons in development of the adult olfactory circuitry. © 2012 Wiley Periodicals, Inc. Develop Neurobiol 73: 107–126, 2013

Keywords: Drosophila Sox gene; olfactory circuit; antennal lobes; local interneurons

INTRODUCTION

Within the *Drosophila* brain, the two antennal lobes (ALs) constitute the primary olfactory relay centers; they are each composed of ~ 50 distinct glomeruli. Within each glomerulus, axons from a discrete class of olfactory receptor neurons (ORNs) synapse onto both specific second order projection neurons (PNs)

and intrinsic local interneurons (LNs) (reviewed in Vosshall and Stocker, 2007; Rodrigues and Hummel, 2008). There exist ~150 PNs that are organized into classes based on their dendritic projections into individual glomeruli and their axonal arborizations in the mushroom body and the lateral horn—the secondary olfactory information processing centers in the fly brain. There also exist ~200 local interneurons (LNs) that are intrinsic to the AL; LN neurites may exhibit pan-, multi-, or uni-glomerular innervation patterns (Chou et al., 2010a). LNs modulate ORN/PN interactions and odor representation within the AL (Ng et al., 2002; Wilson et al., 2004; Wilson and Laurent, 2005; Olsen et al., 2007; Shang et al., 2007; Chou et al., 2010a). Strong progress has been made in describing genes that control PN and ORN differentiation and projection patterns (reviewed in Rodrigues and Hummel, 2008), however, much less is known about the molecular mechanisms underlying LN diversity. Furthermore, while LN functions are clearly important for olfactory coding processes (Shang et al., 2007; Chou et al., 2010a; Huang et al., 2010; Yaksi and Wilson, 2010), a specific role for LNs in development of the olfactory circuit has not been established.

In this study, we identify important functions for the *Dichaete* (a.k.a. *D* or *fish-hook*) gene (Nambu and Nambu, 1996; Russell et al., 1996) in LN differentiation and olfactory circuit formation. *Dichaete* is a member of the well-conserved Sox gene family that encodes transcription regulators containing a single High Mobility Group (HMG) domain. Sox genes have important roles in many early developmental processes and disruptions in human Sox genes are associated with developmental disorders and cancer (reviewed in Dong et al., 2004; Kiefer, 2007; Lefebvre et al., 2007; Chew and Gallo, 2009). Interestingly, mammalian homologs of *Dichaete*, such as Sox 2 and Sox 3, are expressed in olfactory bulb neural precursors and granule cells (Brazel et al., 2005; Wang et al., 2006). However, functions for these genes in olfactory circuit assembly have not been determined. In this study we show that Dichaete protein is expressed in two prominent clusters of ~225 LAAL neurons located adjacent to the ALs in the adult fly brain. These clusters include both cholinergic and GABAergic LNs, as well as ring neurons of the central complex. Interestingly, expression of Dichaete is not detected in either mature or developing PNs or in developing antennal ORNs. Analysis of viable *Dichaete* alleles revealed disruptions in specific PN dendritic innervation patterns within the AL, and disorganization of discrete glomeruli. In addition, the *Dichaete* mutant brains also exhibited altered PN

axonal projections to secondary olfactory processing centers. The lack of Dichaete expression in PNs and analysis of *Dichaete* null mutant PN clones suggest that Dichaete has noncell-autonomous functions important for proper elaboration of PN processes. Taken together, our data suggest that functions of *Dichaete* in LNs may influence PN development, and imply a novel role for LNs in assembly of the adult olfactory circuit.

MATERIALS AND METHODS

Fly Genetics

Drosophila stocks were reared at 25°C under standard laboratory conditions. The wild type strain used was Canton S. Excision of the viable P[rj375] P element (Nambu and Nambu, 1996) was used to generate candidate *Dichaete* mutant alleles. Approximately 100 lines were identified which exhibited a loss of the $rosy^+$ eye color marker on the PZ P element. These lines were then tested for viability as homozygotes and as transheterozygotes with the D^{87} null allele (Nambu and Nambu, 1996). Two alleles, D^{107} and D^{175}, were isolated that were partially viable as homozygotes but exhibited much reduced survival in trans with D^{87}. Balanced D^{107}/TM3,Sb and D^{175}/TM3,Sb strains were generated and used along with a previously isolated semiviable D^{89}/TM3,Sb strain as well as the D^{87}/TM3,Sb and In(3L)D^3/Df(3L)Ly *Dichaete* null alleles (Sanchez-Soriano and Russell, 2000) to assess the viability of various homozygotic or transheterozygotic combinations of *Dichaete* mutations. To determine the extent of viability, complementation crosses between balanced *Dichaete* mutations were performed and the number of nonbalancer progeny adults was divided by the total number of progeny adults. This value was multiplied by 100 to derive a percentage. This percentage was then divided by the expected percent (33%) of nonbalancer progeny from such a cross if the mutation is fully viable. This value was multiplied by 100 to derive a final percent viability. In this scheme, a fully viable mutant would exhibit 100% viability.

Markers for Olfactory System Neurons

All fly strains were obtained from the Bloomington *Drosophila* Stock Center unless otherwise indicated. Neurite projections were visualized using the *UAS-mCD8:GFP* reporter, and nuclei using the *UAS GFP:lacZ_{nls}* reporter. *Elav-GAL4* (Yao and White, 1994) was used to label all post-mitotic neurons and *ChA-GAL4* (Salvaterra and Kitamoto, 2001) to label all cholinergic neurons. *c547-GAL4* (Renn et al., 1999) was used to label central complex ellipsoid body ring neurons. The enhancer trap line *OK107-GAL4* was used to label all *eyeless* expressing cells.

The following *GAL4* lines were used to label subsets of PNs: *GH146-GAL4* (Stocker et al., 1997), *Mz19-GAL4* (Ito et al., 1997; Jefferis et al., 2004), *NP 6115-GAL4*, *acj6-*

GAL4, and *Mz699-GAL4* (Lai et al., 2008). LN subsets were marked by *GAD-1-GAL4* (Ng et al., 2002), *KL107-GAL4, krasavietz-GAL4* (Shang et al., 2007), *c305a-GAL4* (Krashes et al., 2007), *LN1-GAL4* and *LN2-GAL4* (Das et al., 2008). The enhancer trap line *pebbled-GAL4* (Sweeney et al., 2007) was used as a maker for all ORNs, and the promoter-fusion lines *Or-67d-GAL4*, *Or-47b-GAL4* (Vosshall et al., 2000; Fishilevich and Vosshall, 2005), *Or-88a-GAL4* (Komiyama et al., 2004) were used to label specific ORN classes.

The following recombinant chromosomes were generated: *c305a-GAL4*, *UAS-mCD8:GFP*, *Or88a-GAL4*, *UAS-mCD8:GFP*, *Or47b-GAL4*, *UAS-mCD8:GFP* (all on chromosome 2), and D^{87}, *FRT 2A* (on chromosome 3L).

MARCM

Mosaic analyses were performed using *GH146-GAL4* and a D^{87}, *FRT2A* strain according to procedures described in Wu and Luo (2006a).

Molecular Mapping of the P[rJ375] Insertion Site and Excisions in D Mutants

Inverse PCR was performed on genomic DNA isolated from 25–30 P[rJ375] adult flies as described in Mathew et al. (2002). The following primer sequences were used:

- P 5′ sense = 5′-CGCTGTCTCACTCAGACT CAATAC -3′,
- P 5′ rev = 5′-AACCCTTAGCATGTCCGTGG -3′.

To define the excisions in the novel *Dichaete* mutant alleles, genomic DNA was isolated from 25-30 homozygous male D^{107}, D^{175}, and D^{89} mutants with the Qiagen Blood and Tissue Extraction Kit (Qiagen, Valencia CA) using the manufacturer's protocol. Aliquots of the isolated genomic DNA were used in PCR reactions with the following primers:

- xcis4 = 5′-CTGACTACAGAGTACACATAG AGAACGG-3′,
- xcis3 = 5′-TTCTTACCTGGGAGAGAGCTG CG-3′,
- xcis2 = 5′-CCCAGCCTCTATCCCGCTCGC AC-3′,
- xcis1 = 5′-CTTTGCGGTGCGTAGTCCTCCA AG-3′,
- rJ-1f = 5′-CGGCTTCGTCTGGGACTGG-3′
- rJ-3f = 5′-GGGGATCCGTCGACTAAGGCCA AAG-3′
- rJ-5f = 5′-CACTCCTTCCAGGTGCCTCCAG-3′
- rJ-6r= 5′-CGGCTTCGTCTGGGACTGG-3′.

PCR reaction products were analyzed via agarose gel electrophoresis, purified via QIAquick gel purification kits (Qiagen, Valencia CA) and subjected to DNA sequence analysis (Davis Sequencing, Davis CA) to identify the excised DNA associated with each mutant allele.

Immunocytochemistry

The nervous systems of 3–5 day adults or staged pupae were dissected and processed for whole-mount immunocytochemistry using procedures described in Wu and Luo (2006b). Primary antibodies used in this study include rabbit anti-Dichaete serum (1:1000 dilution; Ma et al., 1998), mouse monoclonal 9F8A9 (anti-ELAV) (1:4 dilution; Developmental Studies Hybridoma Bank, IW), mouse monoclonal anti-Acj6 (1:4 dilution; Developmental Studies Hybridoma Bank, IW), and mouse monoclonal anti-β-Gal (1:1000 dilution; Promega Corp., WI). The following fluorescent conjugated secondary antibodies were used to visualize immune complexes: FITC-conjugated Donkey anti-Rabbit, Cy3-conjugated Donkey anti-Rabbit, FITC-conjugated Donkey anti-Mouse, Cy3-conjugated Donkey anti-Mouse, FITC-conjugated Donkey anti-Rat (Jackson ImmunoResearch, PA). Each secondary antibody was used at a 1:200 dilution. Images were collected on a Zeiss LSM 510M laser scanning confocal microscope at the UMass Central Microscopy Facility (http://www.bio.umass.edu/microscopy/). Confocal stacks were obtained at 0.5 μm or 1 mm spacing and processed using ImageJ (NIH) and Adobe Photoshop software.

RESULTS

Dichaete Protein is Expressed in Local Interneurons of the Adult Olfactory System

To analyze Dichaete expression in the adult CNS, anti-Dichaete immunostaining was performed on dissected tissues from 3- to 5-day-old wild type flies. Prominent Dichaete expression was detected in a large number of cells in the medulla layer of the optic lobes [Fig. 1(A)]. These cells included both neurons and glia and some Dichaete-expressing cells coexpress the *Drosophila* Pax-6 homolog, Eyeless (data not shown). Within the central brain, Dichaete expression was observed in scattered cells in the ventral and dorsal/medial regions, and in three prominent paired clusters of cells [Fig. 1(A)]. One cluster is
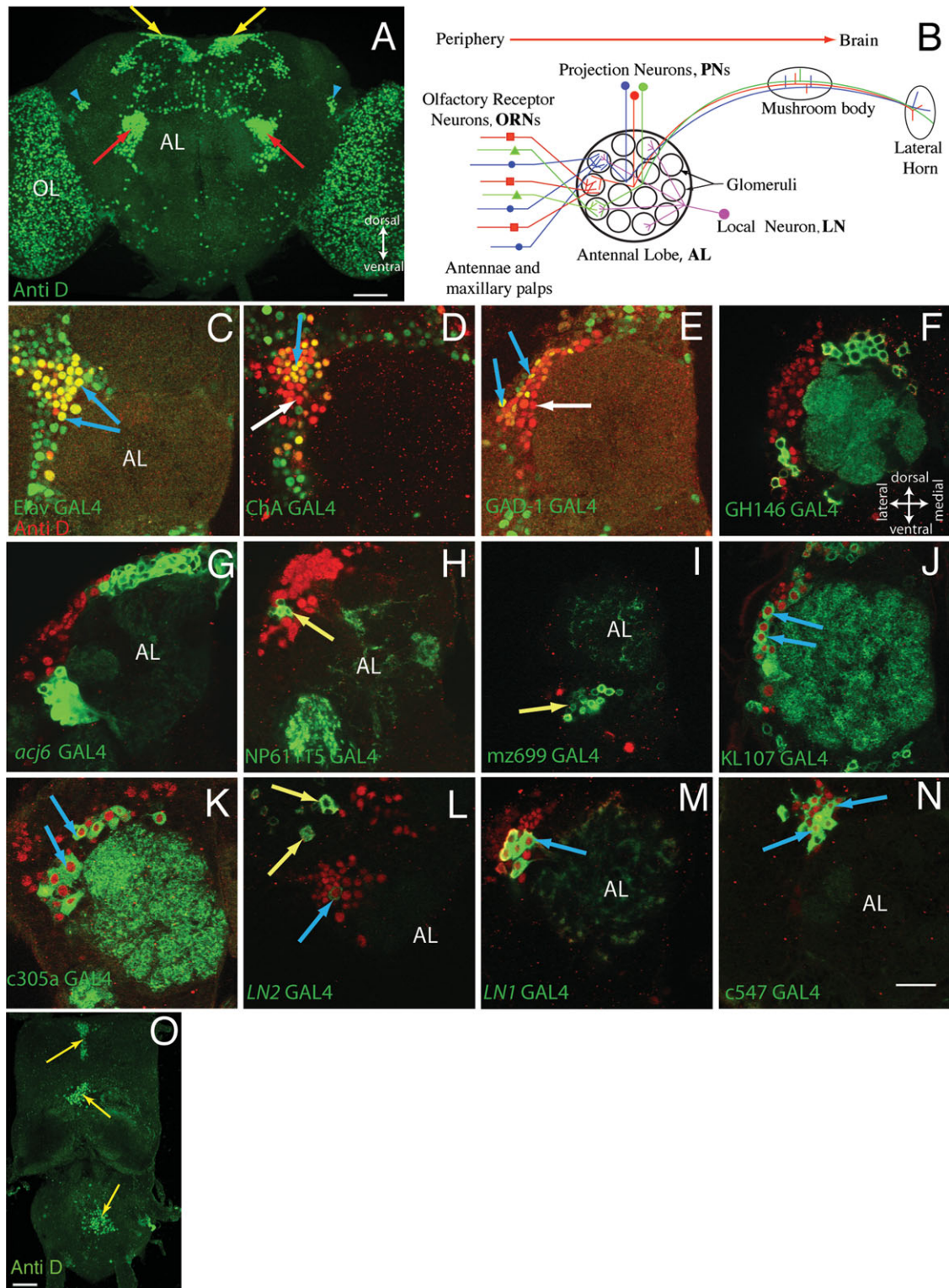
Figure 1

located in the dorsal protocerebrum and extends ventrally from the dorsal margin of the brain. Another is positioned dorsal/lateral, near the boundary with the optic lobes. The third cluster is located adjacent and lateral to each antennal lobe (AL). We hereafter refer to these AL-associated clusters as LAAL (Lateral and Adjacent to Antennal Lobe) cells. Cell counts indicated a total of $\sim$225 Dichaete-expressing cells per LAAL cluster. The location of these cells suggested a potential role for Dichaete in assembly and/or function of the adult olfactory circuit [Fig. 1(B)] and we therefore sought to further characterize the LAAL cells. Double labeling experiments were performed using an anti-Dichaete serum in conjunction with several *GAL4* lines that label different cell types within the central brain [Fig. 1(C–K)]. The LAAL cells all correspond to neurons as they all express *elav-GAL4*, a marker for differentiated neurons [Fig. 1(C)]. Many LAAL cells also express *ChA-GAL4* (Salvaterra and Kitamoto, 2001) identifying them as excitatory cholinergic neurons [Fig. 1(D)]. A smaller proportion of LAAL cells express *GAD1-GAL4* [Fig. 1(E)], identifying them as GABAergic inhibitory neurons (Hamasaka et al., 2005). The position of the LAAL cell bodies and their neurotransmitter expression profile suggested that they correspond to a subset of projection neurons (PNs). However, none of the LAAL cells express *GH146-GAL4* [Fig. 1(F)], a marker that

drives expression in $\sim$2/3 of all PNs (Jefferis et al., 2001). The LAAL cells also do not correspond to other PN types, as indicated by their lack of expression of *acj6-GAL4*, *NP6115-GAL4*, or *Mz699-GAL4* [Fig. 1(G–I)] that together label most/all of the *GH146-GAL4*-negative PNs (Lai et al., 2008). Thus, Dichaete is not expressed in any adult PNs, although the LAAL cells are positioned between *GH146-GAL4*-expressing lPN and adPN clusters.

Another possibility is that the LAAL cells correspond to a heterogeneous set of local interneurons (LNs) that project to some or all glomeruli to modulate interactions between the PNs and olfactory receptor neurons (ORNs). Recent studies have identified a number of *GAL4* lines, e.g., *c305a-GAL4*, *GAD1-GAL4*, *KL107-GAL4*, *krasavietz-GAL4*, *LN1-GAL4*, and *LN2-GAL4* that label discrete subsets of LNs (Krashes et al., 2007; Shang et al., 2007; Das et al., 2008). These LNs may be cholinergic, GABAergic, or express other neurotransmitter phenotypes. Most, though not all of the cells labeled by these LN *GAL4* lines coexpress Dichaete [Fig. 1(J–N)], indicating that a significant proportion of LAAL cells correspond to LNs. Finally, a small subset of the LAAL cells express *c547-GAL4*, a marker that labels the ring neurons of the central complex ellipsoid body (Renn et al., 1999). Thus, the LAAL cells constitute a diverse population of cells, minimally consisting of a

Figure 1 Dichaete protein is expressed in adult olfactory local neurons. A: Confocal *z*-projection through a whole-mount adult brain immunostained with an anti-Dichaete antibody revealed Dichaete expression (green) in several discrete sites in the adult central brain and optic lobes (OL). Prominent Dichaete expression was detected in a cluster of LAAL cells (red arrows). B: Schematic of the *Drosophila* olfactory system, adapted from Komiyama et al. (2003). C–N: Single-confocal sections characterizing the LAAL cells by double-label immunocytochemistry with anti-Dichaete (red) and several cell-type specific markers (green). C: The LAAL cells are all neurons as they express *Elav-GAL4*, a marker for differentiated neurons. D: Many LAAL cells are cholinergic as they co-express *ChA-GAL4*, while other LAAL cells (E) are GABAergic and express *GAD1-GAL4*. Green in (C–E) is GFP:*lacZ*$_{nls}$ driven by the respective drivers. F–I: The LAAL cells are not PNs as they do not express *GH146-GAL4* (F), *acj6-GAL4* (G), *NP 6115-GAL4* (H) or *Mz699-GAL4* (I). J–L: Many of the LAAL cells are cholinergic LNs as they coexpress *KL107-GAL4* (J), *LN1-GAL4* (L), and *c305a-GAL4* (K). A few LAAL cells express *LN2-GAL4* (L) or LN1-GAL4 (M). (N) Some of the LAAL cells are central complex ellipsoid body neurons as they express *c547-GAL4*. (O) Anti-Dichaete immunostaining of the ventral ganglion. Note three prominent clusters of Dichaete-expressing cells (green) along the midline. Green in (F–N) is mCD8GFP expressed via the respective *GAL4* drivers. Blue arrows in (C–N) highlight cells that coexpress Dichaete and various markers, white arrows in (D) and (E) highlight Dichaete-expressing cells that do not coexpress the respective markers, and yellow arrows in (H–N) highlight cells that express *GAL4* but are not D immunoreactive. Only the left antennal lobe is shown in (C–N), these panels are oriented as shown in F. Scale bar in (A) is 40 μm, and for (C–N) is 20 μm as shown in (N). Genotypes depicted: Canton S (A), *elav-GAL4;UAS-GFP*::*lacZ*$_{nls}$ (C), *w; ChA-GAL4, UAS-GFP*::*lacZ*$_{nls}$ (D), *w; GAD1-GAL4, UAS-GFP*::*lacZ*$_{nls}$ (E), *yw; GH146-GAL4, UAS-mCD8GFP* (F), *acj6-GAL4; UAS-mCD8GFP* (G), *NP 6115-GAL4 / UAS-mCD8GFP* (H), *yw; UAS-mCD8GFP/CyO; Mz699-GAL4* (I), *KL107-GAL4; UAS-mCD8GFP; c305a-GAL4, UAS-mCD8GFP* (K), *LN2-GAL4, UAS-mCD8GFP* (L), *LN1-GAL4 / UAS-mCD8GFP* (M), *c547-GAL4, UAS-mCD8GFP* (N).

mixture of excitatory and inhibitory LNs, and central complex ring neurons.

Dichaete expression was also detected in cells of the ventral (thoracicoabdominal) ganglion. Within the ventral ganglion, Dichaete expression was detected in three prominent midline clusters of several dozen cells each [Fig. 1(O)]. Two of these clusters are located between each of the thoracic neuromeres and one is located centrally within the fused abdominal neuromeres. Most or all of these Dichaete-expressing cells co-express Elav (data not shown), indicating they are neurons.

Isolation of Semilethal *Dichaete* Mutant Alleles

Given the proximity of Dichaete-expressing LAAL cells to the antennal lobes and well-documented functions of Dichaete in embryonic nervous system development (Nambu and Nambu, 1996; Soriano and Russell, 1998; Sanchez-Soriano and Russell 2000; Ma et al., 2000; Overton et al., 2002; Buescher et al., 2002; Zhao and Skeath, 2002; Zhao et al., 2007), we investigated the possibility that Dichaete functions might also be required for proper development of the adult olfactory system. *Dichaete* null mutants are embryonic lethal, therefore, to investigate post-embryonic requirements of Dichaete function we generated novel viable *Dichaete* alleles by imprecise excision of the P[rJ375] P element. The parental P element strain, P[rJ375], is a fully viable *Dichaete* enhancer trap insertion that displays lacZ expression in the embryo and larva that mimics the native *Dichaete* gene (Nambu and Nambu 1996; Mukherjee et al., 2000). However, we determined that P[rJ375] does not exhibit expression in the adult CNS. Thus, the P[rJ375] insertion is refractile to the regulatory elements that control adult brain expression of *Dichaete*. Several previously generated *Dichaete* reporter strains (Sanchez-Soriano and Russell, 2000; Venken et al., 2009) also do not drive adult brain expression (data not shown).

The excision screen yielded two novel *Dichaete* alleles D^{107} and D^{175} that are semiviable as homozygotes. One previously isolated allele, D^{89} (Nambu and Nambu, 1996), was also found to be semiviable. As homozygotes, D^{89}, D^{107}, and D^{175} mutants exhibited 8.9%, 76.1%, and 6.2% viability respectively. These three mutant alleles all exhibited greatly reduced viability as transheterozygotes with the D^{87} or D^3 null alleles [Fig. 2(A)]. Thus, D^{89}/D^{87} animals exhibited full lethality while D^{89}/D^3 exhibited 2.7% viability (see MATERIALS AND METHODS for definition). D^{107}/D^{87} animals were 12.2% viable and D^{107}/D^3 were

14.4% viable. D^{175} exhibited 1.0% viability over D^{87} and 6.4% viability with D^3. Importantly, the D^3 mutation was isolated in an independent genetic background (Russell et al., 1996) from D^{107}, D^{175}, and D^{89}, indicating the reduced viability of the novel mutant alleles is due to specific disruption of *Dichaete* gene function. Additional complementation tests were performed to further characterize the viability of the novel *Dichaete* mutant alleles [Fig. 2(A)]. Transheterozygotes of D^{89} and either D^{107} or D^{175} exhibited 71.2% or 32.8% viability respectively, while D^{107}/D^{175} transheterozygotes exhibited 53.9% viability. No anatomical abnormalities were observed in any of the surviving homozygote, heterozygote, or transheterozygote *Dichaete* mutant flies.

To clarify the basis for reduced viability, we characterized the molecular lesions associated with the D^{107}, D^{175}, and D^{89} excision alleles. Inverse PCR and DNA sequence analysis indicated that the viable parent P[rj375] strain (Nambu and Nambu, 1996) contains an insertion of the 14.5 kb PZ P element into the 5′-UTR of the *Dichaete* gene contained on exon 2 [Fig. 2(B)]. The insertion site is located 341 bp upstream of the predicted translation initiation site. PCR primers designed to amplify genomic sequences flanking the insertion site as well as within the PZ P element were used to amplify genomic DNA from D^{107}, D^{175}, and D^{89} homozygote adults. Surprisingly, none of the three novel *Dichaete* alleles are associated with any loss of genomic DNA within or nearby the *Dichaete* locus. However, each allele does contain significant internal loss of P element sequences [Fig. 2(B)]. The D^{107} and D^{89} alleles both contain a single deletion within the PZ P element, spanning 9.6 kb for D^{89} and 10.1 kb for D^{107}; the right breakpoints are essentially identical at 1-bp apart. In contrast, the D^{175} allele contains two internal deletions that together span 9.3 kb; the leftmost breakpoint extends approximately 2–3 kb further than that of D^{107} or D^{89} and the rightmost breakpoint is the same as D^{107} [Fig. 2(B)]. The D^{175} mutation also removes a portion of the *lacZ* marker gene contained within the PZ P element. Thus, the rightmost breakpoint for each of these alleles is essentially identical and removes most of the 3′ P element repeat. In contrast, the left-most breakpoint differs in all three alleles, extending within 4–5 kb of the P element 5′ end. These data suggest that the novel *Dichaete* alleles correspond to regulatory mutations that affect specific aspects of the normal pattern of Dichaete expression.

To determine how the novel *Dichaete* mutations may alter Dichaete expression in the adult brain, anti-Dichaete immunocytochemistry was performed on D^{107} and D^{89} mutants [Fig. 2(C,D)]. Compared with
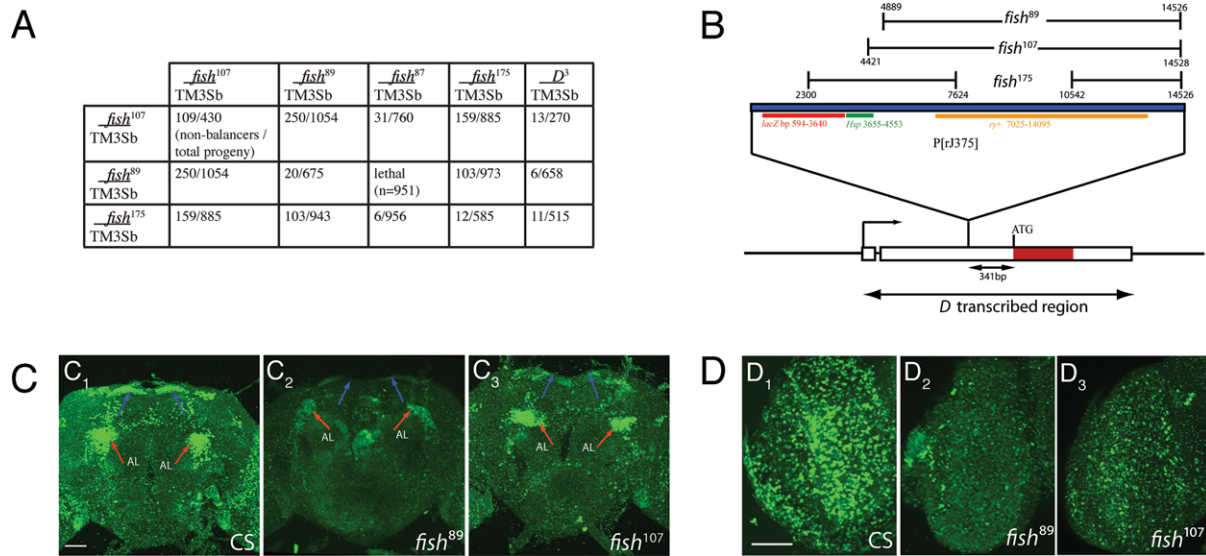
Figure 2 Characterization of novel viable *Dichaete* alleles. A: Complementation tests with the viable *Dichaete* excision alleles and *Dichaete* null alleles. The D^{89}/TM3,Sb, D^{107}/TM3,Sb, and D^{175}/TM3,Sb lines were crossed to each other and to the D^{87}/TM3,Sb and D^3/TM3,Sb lines. The adult progeny were scored and the number of homozygous or transheterozygous mutants (nonbalancer flies : numerator) and total progeny flies (balancer + nonbalancer : denominator) determined. The D^{89}, D^{107}, and D^{175} alleles all exhibited partial viability (see MATERIALS AND METHODS) as homozygotes (8.9% viability, 76.1% viability, or 6.2% viability respectively) or in trans to each other (71.2% viability for D^{89}/D^{107}; 32.8% viability for D^{89}/D^{175}; and 53.9% viability for D^{107}/D^{175}). However, each allele exhibited greatly reduced viability in transheterozygote combinations with the D^{87} and D^3 null alleles (full lethality for D^{89}/D^{87}; 2.7 % viability for D^{89}/D^3; 12.2% viability for D^{107}/D^{87}; 14.4% viability for D^{107}/D^3; 1.9 % viability for D^{175}/D^{87}; and 6.4 % viability for D^{175}/D^3). B: Molecular mapping of the D^{89}, D^{107}, and D^{175} P element excision alleles. The precise of location of the breakpoints in the three alleles is diagrammed above the P[rJ375] P element (blue box) insertion into the 5′-UTR of the *Dichaete* gene. Positions of the *lacZ* and *rosy* (ry^+) marker genes are indicated. *Dichaete* gene exons are indicated by white boxes with the coding region (red). The *Dichaete* transcription start site is marked with an arrow, and ATG marks the translation start site. C: *Dichaete* mutants exhibit defects in Dichaete expression in the central brain. (C_1-C_3) are confocal z-projections of adult brains from wild type (C_1), D^{89} (C_2), and D^{107} (C_3) animals immunostained with an anti-Dichaete antibody (green). Dichaete expression was strongly reduced throughout D^{89} brains compared to wild type controls (compare C_2 with C_1), and moderately reduced in D^{107} brains (compare C_3 with C_1). The LAAL cells appeared displaced medially and dorsally in both D^{89} and D^{107} brains (red arrows in C_2 and C_3), and Dichaete expression was absent in the dorsal protocerebrum in ∼50% of both D^{89} and D^{107} mutant brains (blue arrows in C_2 and C_3). All panels are oriented as in C_3, with the scale bar shown in C_1 representing 40 μm. D: Dichaete expression in the optic lobes is severely reduced in D^{89} (D_2) and D^{107} (D_3) mutants compared to wild type controls (D_1). (D_1-D_3) are confocal *z*-projections through optic lobes immunostained with anti-Dichaete (green). All panels are oriented as in (D_3), with the scale bar shown in (D_1) representing 40 μm. Genotypes depicted: Canton S (C_1, D_1), D^{89} (C_2, D_2), D^{107} (C_3, D_3). [Color figure can be viewed in the online issue, which is available at wileyonlinelibrary.com.]

wild type controls, Dichaete protein expression was strongly reduced throughout D^{89} mutant brains, including the LAAL cells [Fig. 2($C_{1,2}$)]. Dichaete expression was less affected in D^{107} mutant brains and the mutant LAAL cells maintained significant Dichaete expression [Fig. 2($C_{1,3}$)]. Interestingly, in both the D^{89} and D^{107} mutant brains, the LAAL clusters appeared reduced compared to the wild type and exhibited an altered localization, displaced dorsally and medially from the AL [Fig. 2($C_{1,3}$)]. In addition, in ∼50% of both D^{89} and D^{107} mutant brains, there were also fewer Dichaete-expressing cells in the dorsal protocerebrum [Fig. 2(C_{1-3})]. Dichaete expression was also examined in the optic lobes of D^{89} and D^{107} mutants [Fig. 2(D)]. Compared with wild type controls [Fig. 2(D_1)], anti-Dichaete immunostaining indi-

cated a reduction of Dichaete-expressing cells in both D^{89} [Fig. 2(D$_2$)] and D^{107} [Fig. 2(D$_3$)] mutant optic lobes. These findings are consistent with either defects in the formation and/or survival of optic lobe cells in D^{107} and D^{89} mutants, or a loss of Dichaete expression in specific subsets of mutant optic lobe cells. Overall, the viable Dichaete mutations clearly disrupt the normal Dichaete expression patterns in the adult brain in a mosaic fashion.

Viable *Dichaete* Mutants Exhibit Aberrant PN Projections

The location of the displaced LAAL cells in D^{107} and D^{89} mutant brains [Fig. 2(C)] resembles the expression domain of Acj6, a POU domain transcription factor expressed in adPNs (Komiyama et al., 2003; Lai et al., 2008). Thus, one possibility is that in *Dichaete* mutants the LAAL cells might be transformed into Acj6-expressing adPNs. To test this hypothesis, double-label immunostaining with anti-Dichaete and anti-Acj6 antibodies was performed on wild type and *Dichaete* mutant brains [Fig. 3(A)]. In wild type brains the LAAL clusters are lateral to the AL, positioned between, and not overlapping with, the dorsal and lateral/ventral clusters of Acj6-expressing neurons [Fig. 3(A$_1$)]. In D^{107} and D^{89} mutant brains, the Dichaete-expressing LAAL cells are displaced dorsally and medially into a region that normally includes the dorsal expression domain of Acj6 [Fig. 3(A$_{2,3}$)]. This displacement was often associated with a reduction or elimination of dorsal Acj6-expressing PNs, suggesting defects in Acj6 PN formation or survival. D^{107} and D^{89} mutant brains also exhibited altered locations of Acj6 PNs, with lateral/ventral Acj6 PNs often dispersed more dorsally into the region normally occupied by the LAAL cells. Thus, the positions of Dichaete- and Acj6-expressing cells are both altered. Strikingly, no overlap was ever detected in the expression of these genes; Dichaete and Acj6 expression domains were always mutually exclusive. While there is clearly not a complete transformation of all mutant LAAL cells into Acj6-PNs, alterations in the positions and numbers of both cell types may indicate altered identities for a subset of these neurons.

Given the disruption of Acj6-expressing PNs in *Dichaete* mutant brains, we examined if PN dendritic projections into the AL might also be altered. To identify potential PN targeting defects we utilized *Mz19-GAL4* to drive *UAS-mCD8:GFP* expression in a small subset ($\sim$6 adPNs and $\sim$7 lPNs) of PNs that all express both Acj6 and *GH146-GAL4*. *Mz19-GAL4* PN dendrites arborize in the DA1 and VA1d glomeruli located in the anterior AL, and the posteriorly

located DC3 glomerulus (Ito et al., 1997; Jefferis et al., 2004). Compared with wild type adult brains [Fig. 3(B$_1$)], D^{89} [Fig. 3(B$_2$–B$_4$)] and D^{107} [Fig. 3(B$_5$–B$_6$)] mutant brains exhibited distinct defects in *Mz19-GAL4* PN dendritic patterns. In some mutants [Fig. 3(B$_2$, B$_5$)] only a single glomerulus was innervated. This glomerulus was often aberrantly shaped, but generally located in a position consistent with DA1. This phenotype was frequently associated with a loss of some or all *Mz19-GAL4* adPNs. In other mutants the *Mz19-GAL4* PN dendrites exhibited ectopic innervation of glomeruli that were generally adjacent to VA1d [Fig. 3(B$_{3,4,6}$)], and frequently included VA1lm [Fig. 3(B$_{3,4}$)]. The two phenotypes were observed at similar frequencies, and together, were seen in $\sim$35% of D^{89} ($n = 60$) and $\sim$25% of D^{107} ($n = 52$) brains. Unlike wild type brains where the *Mz19-GAL4* PN dendrites generally filled the entire volume of a glomerulus, in D^{89} and D^{107} mutants the dendrites were often spatially restricted within a glomerulus [Fig. 3(B$_4$)]. Similar defects in *Mz19-GAL4* PN dendritic patterns were observed in D^{89}/D^3 transheterozygotes (data not shown), confirming that the mutant phenotypes correspond to specific disruption of *Dichaete* gene function. Thus, Dichaete function appears to be important for the proper dendritic projections of *Mz19-GAL4* PNs.

We also analyzed the axonal trajectories of *Mz19-GAL4* PNs in *Dichaete* mutants. In wild type brains, axons from the two *Mz19-GAL4* PN clusters fasciculate together and arborize in the mushroom bodies (MBs) and lateral horn (LH) via the inner antenno-cerebral tract (iACT) [Fig. 4(A$_1$,A$_1$')]. In contrast, in $\sim$10% of D^{89} mutant brains ($n = 30$) *Mz19-GAL4* PN axons followed abnormal routes to the LH [Fig. 4(A$_2$,A$_2$',A$_3$,A$_3$')]. The aberrant axonal trajectories resembled the middle antenno-cerebral tract (mACT), except that the mutant PN axons extended a long offshoot from this mACT-like path that arborized in the MB. In contrast, in 50% ($n = 16$) of the D^{89} mutant brains, *Mz19-GAL4* PN axons followed the wild type path (iACT) to the LH [Fig. 4(B,B$_1$,B$_1$')], but exhibited atypical secondary and/or tertiary branches within the LH [Fig. 4(B$_2$,B$_2$',B$_3$,B$_3$')].

In some cases these mutant branches extended dorsally along the lateral edge of the LH [Fig. 4(B$_3$, B$_3$')]. Thus, in addition to defects in PN dendritic targeting, PN axons follow aberrant paths to higher olfactory centers and exhibit abnormal arborization within the LH. The distinct defects in PN dendrites and axons could reflect disruption of a common Dichaete function that is required for two separate PN differentiation processes, or disruptions of different Dichaete functions required in dendrites or axons.
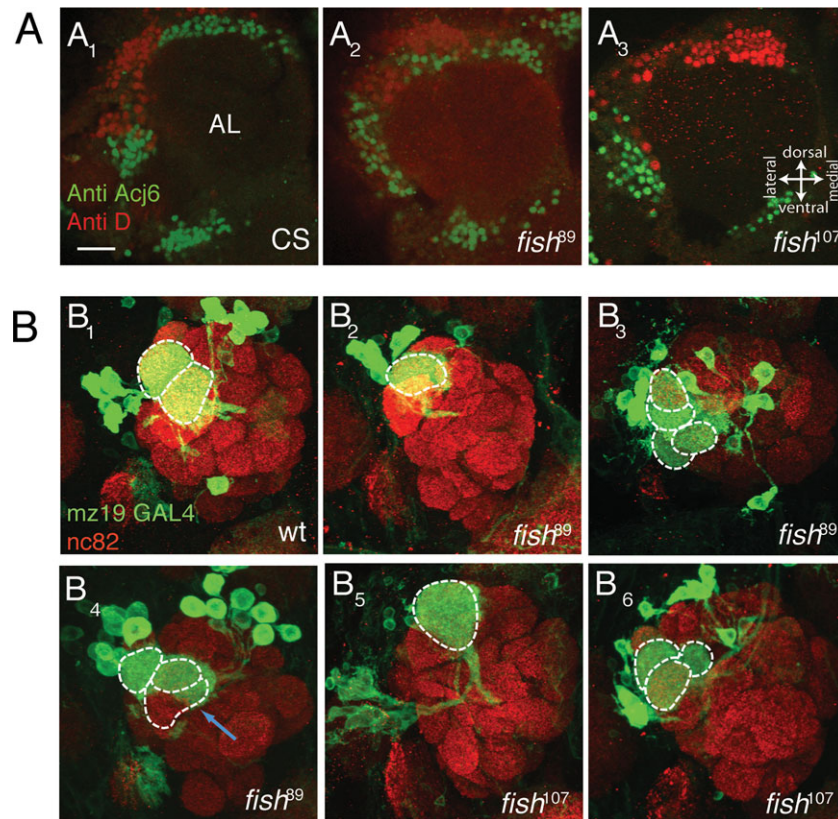
Figure 3 Projection neuron organization and dendritic targeting are disrupted in *Dichaete* mutant brains. A: Compared with the wild type (A_1), D^{89} (A_2), and D^{107} (A_3) mutant brains exhibit Dichaete-expressing LAAL cells (red) that are displaced dorsally and medially into a domain normally occupied by the Acj6-expressing adPNs (green). The LAAL displacement in *Dichaete* mutants is accompanied by a concomitant displacement of Acj6 expressing cells, such that the domains of Dichaete and Acj6 remain nonoverlapping. All panels are single confocal sections through the adult AL, oriented as in A_3. The scale bar for all panels (shown in A_1) is 20 μm. B: In the wild type (B_1) mCD8GFP driven by *Mz19-GAL4* (green in all panels) labels two clusters of PNs whose dendrites innervate two glomeruli on the anterior surface of the AL–DA1 and VA1d and one more posteriorly located glomerulus–DC3. In contrast, in 35% of D^{89} and $\sim$25% of D^{107} mutant brains exhibited PN projection defects. *Mz19-GAL4* PN dendrites either innervate a single glomerulus in D^{89} (B_2) and D^{107} (B_5), or they innervate ectopic glomeruli D^{89} ($B_{3,4}$) and D^{107} (B_6). Unlike the wild type, both D^{89} and D^{107} mutant brains occasionally exhibited *Mz19-GAL4* PN dendrites that did not completely fill a glomerulus (e.g., blue arrow in B_4). All panels are anterior views of maximum intensity *z*-projections through the left AL, oriented as in A_3. In all panels glomerular boundaries are outlined (white), mCD8GFP (green) is expressed via *Mz19-GAL4* in a subset of PNs, and anti-nc82 immunostaining (red) labels glomeruli neuropil. The scale bar for all panels (shown in B_6) is 20 μm. Genotypes depicted: Canton S (A_1), D^{89} (A_2), D^{107} (A_3), *y w*; *Mz19-GAL4*, *UAS-mCD8GFP* (B_1), *w*; *Mz19-GAL4*, *UAS-mCD8GFP*; D^{89} (B_2-B_3), *w*; *Mz19-GAL4*, *UAS-mCD8GFP*; D^{107} (B_4-B_5), *w*; *Mz19-GAL4*, *UAS-mCD8GFP*; D^{89} / D^3 (B_6). [Color figure can be viewed in the online issue, which is available at wileyonlinelibrary.com.]

Potential Cell Nonautonomous Functions of Dichaete in PN Differentiation

Because Dichaete expression is not detected in adult PNs, the PN projection defects in *Dichaete* mutant brains suggest either that the *Dichaete* gene is transiently expressed during development of the PN lineage, or that it has cell nonautonomous functions in PN differentiation. As the class-specific sorting of PN dendrites during early pupal development requires transient functions of the Acj6 and Dfr POU domain transcription factors during the first half of pupal development (Komiyama et al., 2003), we tested the possibility that Dichaete might also be transiently
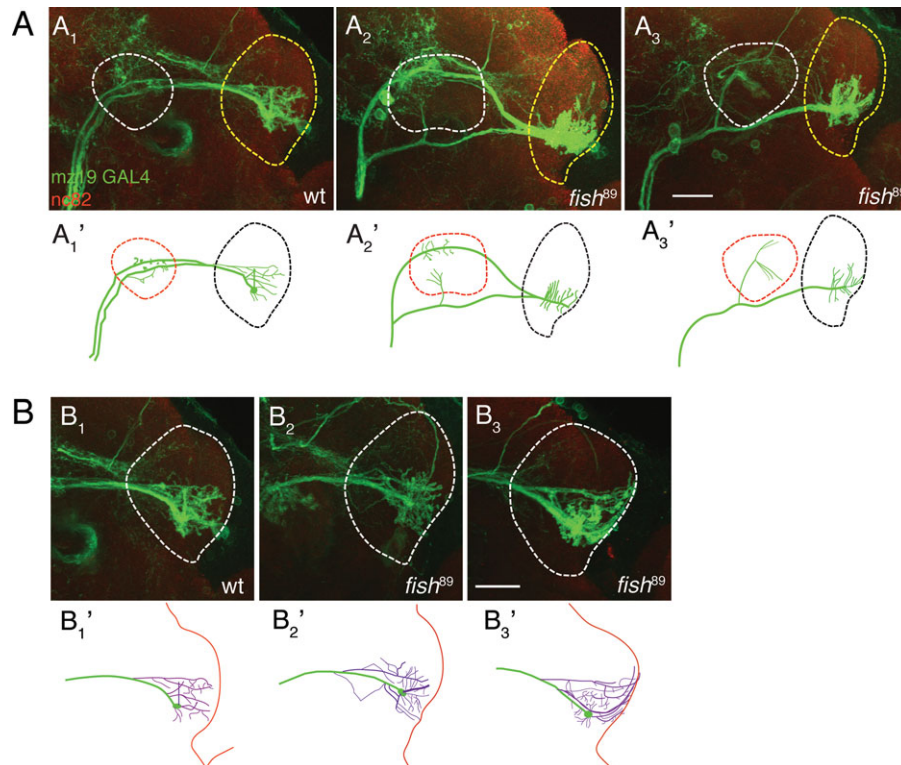
Figure 4   Projection neuron axons are mis-targeted in *D* mutant brains. (A) In D^{89} mutant brains PN axons sometimes follow aberrant paths to the mushroom bodies (MH) and lateral horn (LH). In wild type controls (A_1, schematized in A_1'), *Mz19-GAL4* PN axons fasciculate together and follow the iACT to the MB and LH. In contrast, in $\sim 10\%$ of D^{89} (A_2 and A_3) mutants, (schematized in A_2' and A_3' respectively) these axons take incorrect paths to the LH, elaborating a track that resembles the mACT except that it includes a branch which arborizes in the MB. (A_1-A_3) are posterior views of maximum intensity confocal *z*-projections through the brain oriented as in (A_3). *Mz19-GAL4* driven mCD8GFP expression (green) and anti-nc82 immunostaining (red) is shown. The MB is outlined in (A_1-A_3) (white) and in (A_1' – A_3') (red). The LH is outlined in (A_1-A_3) (yellow) in (A_1' – A_3') (black). The scale bar in A_3 is 20 μm. B: In D^{89} mutant brains PN axons elaborate aberrant arbors in the LH. In wild type controls (B_1, schematized in B_1') *Mz19-GAL4* PN axons exhibit class-specific axonal arbors in the LH. In 50% of D^{89} mutant brains these axons took the normal path to the LH (B_2-B_3, schematized in B_2' and B_3' respectively); however, the pattern of axonal arborization in the LH was frequently disrupted. In a few such cases PN axonal arbors elaborated more secondary branches (B_2, schematized in B_2') in other cases (B_3, schematized in B_3') the secondary branches appeared longer and extended along the edge of the LH. (B_1-B_3) are posterior views maximum intensity *z*-projections of 1 μm spaced confocal stacks through the LH of brains of the indicated genotypes. *Mz19-GAL4* driven mCD8GFP (green) and anti-nc82 immunostaining (red) are presented. (B_1-B_3) are oriented as in (B_3), the scale bar in (B_3) is 20 μm. ($B1'$ – B_3') are schematics of the images in (B_1-B_3) with PN axon tracts (green) and LH outline (red) indicated. Genotypes depicted: *y w*; *Mz19-GAL4*, *UAS-mCD8GFP* (A_1, B_1), *w*; *Mz19-GAL4*, *UAS-mCD8GFP*; D^{89} (A_2-A_3, B_2-B_3).

expressed in PNs during pupation. Anti-Dichaete immunostaining was performed on the brains of developing *GH146-GAL4*, *UAS-mCD8:GFP* pupae at six different time points. These time points ranged from 0 hours after puparium formation (APF) to 51 h APF, at which point PN dendritic sorting and axonal branching are essentially complete (Komiyama et al., 2003; Jefferis et al., 2004). Significantly, no overlap

was ever detected between the expression of Dichaete and GFP at any of the stages of pupal development examined [Fig. 5(A)]. Minimally, this indicates that Dichaete is not transiently expressed in any *GH146-GAL4* PN (including all *Mz19-GAL4* adPNs) during early to mid pupal development. Thus, Dichaete is not expressed in developing or mature PNs. We also tested if Dichaete may be expressed in olfactory re-

ceptor neurons (ORNs) and that disruption of this function interferes with ORN/PN interactions important for PN differentiation. We addressed this via double-label immunostaining using anti-Dichaete and anti-Elav antibodies against antennae isolated from ~ 36 hr APF *pebbled-GAL4*; *UAS-mCD8:GFP* pupae [Fig. 5(B)]. This period corresponds to a critical stage in ORN axon targeting, when ORN classes are sorting into protoglomeruli. No Dichaete expression was detected in the 3rd antennal segment where ORN cell bodies reside - demonstrating that Dichaete is not expressed in ORNs at this stage. Dichaete expression was observed in unidentified non-neuronal cells within the 2nd antennal segment [Fig. 5(B)]. Thus, it appears that Dichaete does not act in developing antennal ORNs to influence elaboration of PN processes.

To further analyze the potential nonautonomous requirement for Dichaete in PN differentiation, MARCM was employed using the D^{87} null allele and *GH146-GAL4*. Analysis of GFP-expressing D^{87} mutant adPN, lPN and vPN Nb clones revealed normal patterns of dendritic arborizations and axon trajectories that were indistinguishable from those of wild type controls [Fig. 5(C)]. Taken together with the observed lack of Dichaete expression in any PNs, the results suggest that the alterations of *Mz19-GAL4* projection patterns in *Dichaete* mutants do not result from disruptions in Dichaete function directly in *Mz19-GAL4* PNs or their neuroblast precursors. Instead, the results are consistent with noncell-autonomous functions of Dichaete in PN development.

These data raise the possibility that developing LNs are critical for PN differentiation. For example, LNs could provide a growth substrate or signal(s) that directs PN outgrowth. Disruptions in LN development or function could subsequently result in abnormal elaboration of PN processes. We therefore examined LN projections and Dichaete expression in wild type and D^{89} and D^{107} mutant brains using anti-Dichaete immunostaining in combination with *c305a-GAL4* and *UAS-mCD8:GFP*. In wild type brains, *c305a-GAL4* labels a large cluster of excitatory LNs located lateral to the AL and their axons fasciculate together to enter the AL [Fig. 6(A_1,B_1)]. Most of the *c305a-GAL4* LNs also express Dichaete. In D^{89} and D^{107} mutant brains, the *c305a-GAL4* LN cell bodies were slightly displaced, occupying more antero-dorsal positions [Fig. 6(A_{2-3},B_{2-3})]. However, the numbers of Dichaete-expressing *c305a-GAL4* LNs in *Dichaete* mutants were comparable to the wild type, and *c305a-GAL4* LN axons exhibited normal projections into the AL. This result suggests that *Dichaete* mutants do not eliminate a LN substrate necessary for elaboration of PN projections. However, the *Dichaete*

mutant LNs could still be defective in providing a signal important for normal PN projections.

Mz19-GAL4 PN Target Glomeruli Are Not Disrupted in *Dichaete* Mutant Brains

The PN dendritic targeting defects in *Dichaete* mutant brains could be an indirect consequence of defects in glomerulus formation. For example, if a single *Mz19-GAL4* target glomerulus fails to form, the corresponding PNs could be eliminated by cell death and the remaining *Mz19-GAL4* PNs may innervate the remaining two target glomeruli. Similarly, if a single *Mz19-GAL4* target glomerulus split into two glomeruli, *Mz19-GAL4* PNs might innervate an ectopic glomerulus. We investigated the integrity of the *Mz19-GAL4* target glomeruli DA1 and VA1d by examining projections of OR67d and OR88a ORNs that respectively project to these sites (Komiyama et al., 2004; Fishilevich and Vosshall, 2005). OR67d axons exhibited normal projections to DA1 in D^{89} ($n = 18$) and D^{107} ($n = 21$) mutant brains [see Fig. 7(A_{1-3})]. *OR67d-GAL4* also labels axons that project to the VA6 glomerulus (Couto et al., 2005; Fishilevich and Vosshall, 2005) that is not innervated by *Mz19-GAL4* neurons [Fig. 7(A_1)]. Innervation of VA6 by *OR67d-GAL4* axons was also unaltered in either D^{107} or D^{89} mutants [Fig. 7($A_{2,3}$)]. In addition, OR88a axons all projected normally to ipsilateral VA1d glomerulus in D^{107} ($n = 23$) and D^{89} ($n = 25$) mutant brains [Fig. 7(B_{1-3})]. Unlike the *Mz19-GAL4* PN dendrites, there were no instances of OR67d or OR88a axons projecting to ectopic glomeruli. This finding argues against the dendritic targeting defects of *Mz19-GAL4* PNs in *Dichaete* mutants being a secondary consequence of glomerular defects. However, because in some *Dichaete* mutant brains *Mz19-GAL* PN dendrites inappropriately innervate the VA1lm glomerulus [see Fig. 3(B_4)], we also examined the axons of OR47b neurons that project to VA1lm [Fig. 7(C_1)]. In $\sim 60\%$ of D^{107} ($n = 12$) and $\sim 50\%$ of D^{89} ($n = 11$) mutant brains OR47b axons exhibited aberrant ipsilateral innervation of both the VA1lm as well as a neighboring glomerulus, possibly VA1d [Fig. 7($C_{2,3}$)]. Thus, at least one ORN class does exhibit targeting defects in *Dichaete* mutants. However, the alterations in OR47b axon targeting are not likely to explain the *Mz19-GAL4* PN defects in *Dichaete* mutants. Thus, it has been shown that *Mz19-GAL4* PN dendrites still target normally to the DA1 and VA1d target glomeruli when OR47b axons mistarget to ectopic glomeruli (Lattemann et al., 2007). Furthermore, OR47b axons target correctly to VA1lm when PN dendrites are mistargeted (Zhu and Luo,
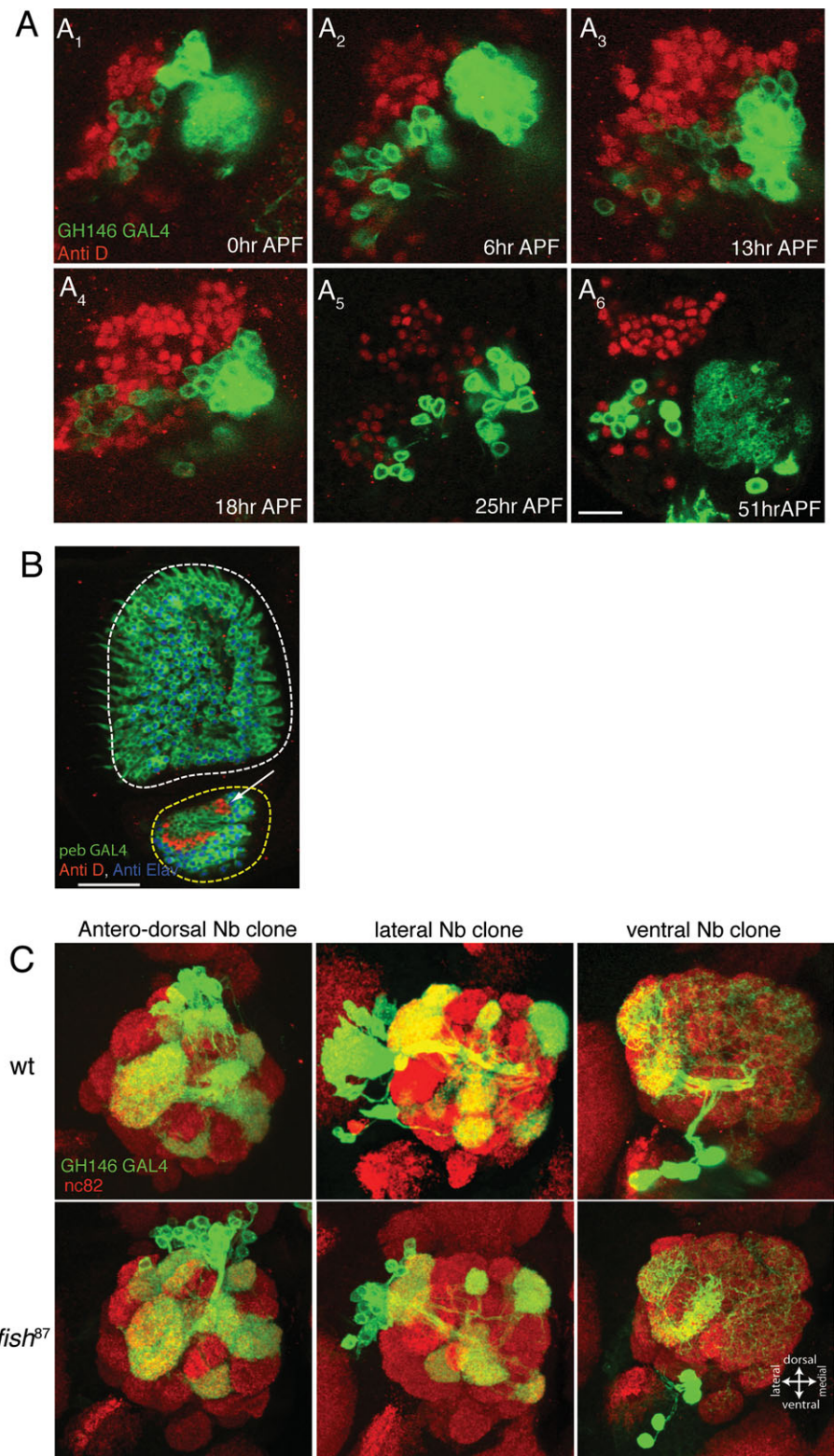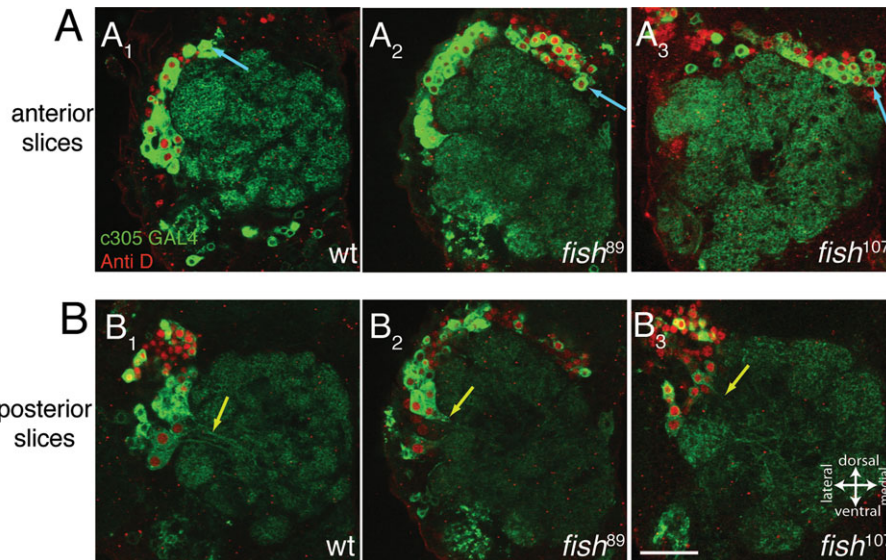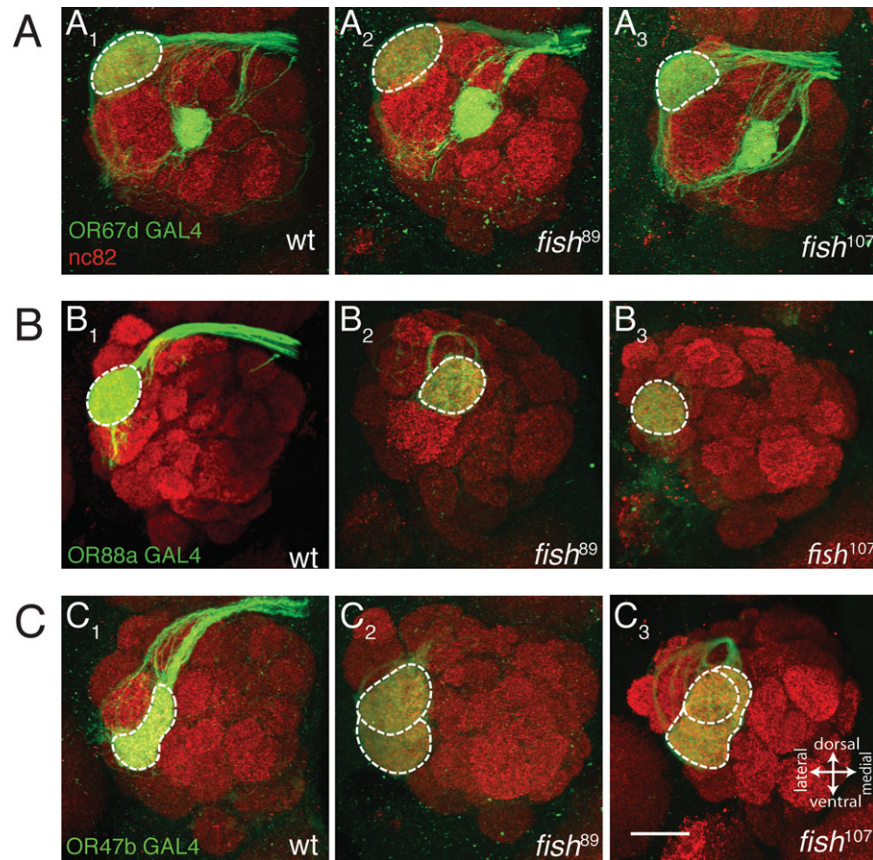
Figure 5

Figure 6 LN development is not dramatically altered in *Dichaete* mutants. In wild-controls (A_1, B_1) LN cell bodies are located lateral to the AL (blue arrow in A_1), and their neurites fasciculate together and project into the AL (yellow arrow in B_1). In D^{89} (A_2,B_2) and D^{107} (A_3, B_3) mutant brains, LN cell bodies are frequently displaced dorsally and medially (blue arrow in A_2, A_3), yet LN axons appear to fasciculate normally and project into the AL (yellow arrow in B_2, B_3). mCD8GFP driven by *c305a-GAL4* (green) and anti-Dichaete immunostaining (red) is presented. All panels are single confocal sections through the AL, oriented as in (B_3), the scale bar in (B_3) is 20 μm. A: Optical sections through the anterior AL are depicted. B: Optical sections through the posterior AL are depicted. Genotypes depicted: *w*; *c305a-GAL4, UAS-mCD8GFP* (A_1, B_1), *w*; *c305a-GAL4, UAS-mCD8GFP*; D^{89} (A_2, B_2), *w*; *c305a-GAL4, UAS-mCD8GFP*; D^{107} (A_3, B_3). [Color figure can be viewed in the online issue, which is available at wileyonlinelibrary.com.]

2004). Interestingly, targeting of specific ORN classes (though not OR47b neurons) was recently shown to be dependent on Hedgehog protein expressed in PNs and other AL-associated neurons (most likely LNs) (Chou et al, 2010b). While the sites of Dichaete function essential for OR47b targeting are still unclear, one possibility is that Dichaete function is required in a recently described class of LNs whose neurites surround DA1, VA1d, and VA1lm (Chou et al., 2010a). In addition, it is also possible that in *Dichaete* mutants there is a conversion of an 88a ORN to a 47b ORN without a concomitant alteration in glomerular connectivity. Thus, in *Dichaete* mutants an ectopic 47b ORN (derived from an 88a

Figure 5 Dichaete is not expressed in developing PNs or ORNs and *Dichaete* null mutant *GH146-GAL4* PN clones exhibit normal dendritic organization. A: Dichaete expression (red) was not detected in developing PNs of pupae at 0 h APF (A_1), 6 h APF (A_2), 13 h APF (A_3), 18 h APF (A_4), 25 h APF (A_5) or 51 h APF (A_6). *GH146-GAL4* PNs are labeled via mCD8GFP (green). B: Dichaete is not expressed in developing antennal ORNs. Dichaete expression (red) is not detected in ORNs (36 h APF) of the third antennal segment (outlined in white), but is expressed in non-neuronal cells in the second antennal segment (outlined in yellow). *pebbled-GAL4* targeted mCD8GFP expression (green) and anti-Elav immunostaining (blue) are presented. A,B: The scale bar corresponds to 40 μm. Genotypes: *yw*; *GH146-GAL4, UAS-mCD8GFP* (A_{1-6}) *peb-GAL4*; *UAS-mCD8 GFP* (B). C: *Dichaete* null mutant PN clones generated via MARCM exhibit normal dendritic targeting. Upper panels: dendrites of antero-dorsal, lateral, and ventral *GH146-GAL4* positive PN neuroblast clones innervate distinct, lineage specific, nonoverlapping sets of glomeruli in wild type (wt) brains. Lower panels: dendrites of antero-dorsal, lateral, and ventral *GH146-GAL4* positive D^{87} *Dichaete* null mutant PN Nb clones exhibit wild type patterns of glomerular innervation. *GH146-GAL4* driven mCD8GFP (green) and anti-nc82 immunostaining (red) are presented. All panels are oriented as in the bottom-right panel. Genotypes depicted: *y w hsFLP*[122] *UAS-mCD8GFP*; *GH146-GAL4, UAS-mCD8GFP*; *FRT2A* (wild type), *yw hsFLP*[122] *UAS-mCD8GFP*; *GH146-GAL4, UAS-mCD8GFP*; D^{87} *FRT2A* (D^{87}).

Figure 7 Targeting of ORN axons is disrupted in *Dichaete* mutant brains in a class-specific fashion. A: OR67d ORNs target target normally in *Dichaete* mutant brains. In wild type brains (A_1) axons of OR67d expressing neurons (green: labeled by anti-GFP antibody in A_1-A_3) target to the DA1 (outlined in white) and VA6 glomeruli. Targeting was not affected in D^{89} (A_2) or D^{107} (A_3) mutant brains. B: OR88a ORN axonal targeting is not affected in *D* mutant brains. In wild type brains (B_1) axons of OR88a expressing neurons (green; labeled by anti-GFP antibody in B_1-B_3) target to the VA1d glomerulus (outlined in white). C: OR47b axons are mistargeted in *Dichaete* mutant brains. In wild type brains (C_1) OR47b ORNs (green: labeled by anti-GFP antibody) target to the VA1l/m glomerulus (outlined in white). In contrast, in ∼60% of D^{89} (C_2) and 50% of D^{107} (C_3) mutant brains, OR47b axonal terminals innervate ectopic glomeruli (outlined in white). Genotypes depicted: *OR67d-GAL4; UAS-mCD8GFP* (A_1), *OR67d-GAL4; UAS-mCD8GFP; D^{89}* (A_2), *OR67d-GAL4; UAS mCD8GFP; D^{107}, w; OR88a-GAL4, UAS-mCD8GFP* (B_1), *w; OR88a-GAL4, UAS-mCD8GFP; D^{89}* (B_2), *w; OR88a-GAL4, UAS-mCD8GFP; D^{107}* (B_3), *w; OR47b-GAL4, UAS-mCD8GFP* (C_1), *w; OR47b-GAL4, UAS-mCD8GFP; D^{89}* (C_2), *w; OR47b-GAL4, UAS-mCD8GFP; D^{107}* (C_3). [Color figure can be viewed in the online issue, which is available at wileyonlinelibrary. com.]

ORN) may still project to the 88a ORN VA1d glomerulus.

Midline Crossing of Specific ORN Axons Is Disrupted in *Dichaete* Mutant Brains

OR67d, OR88a, and OR47b neurons all project axons through the antennal nerve to their target glomeruli in the ipsilateral AL and also extend projections across the midline to innervate corresponding contralateral glomeruli. In *Dichaete* mutant brains, OR67d axons projected normally both ipsilaterally, and across the midline to the contralateral glomeruli [Fig. 8(A_{1-3})]. However, in >40% of *Dichaete* mutant brains, OR88a and OR47b axons failed to cross the midline and remained strictly ipsilateral [Fig. 8(B_{1-3},C_{1-3})]. As Dichaete expression is not detected in ORNs during the period when their axons are sorting into protoglo-
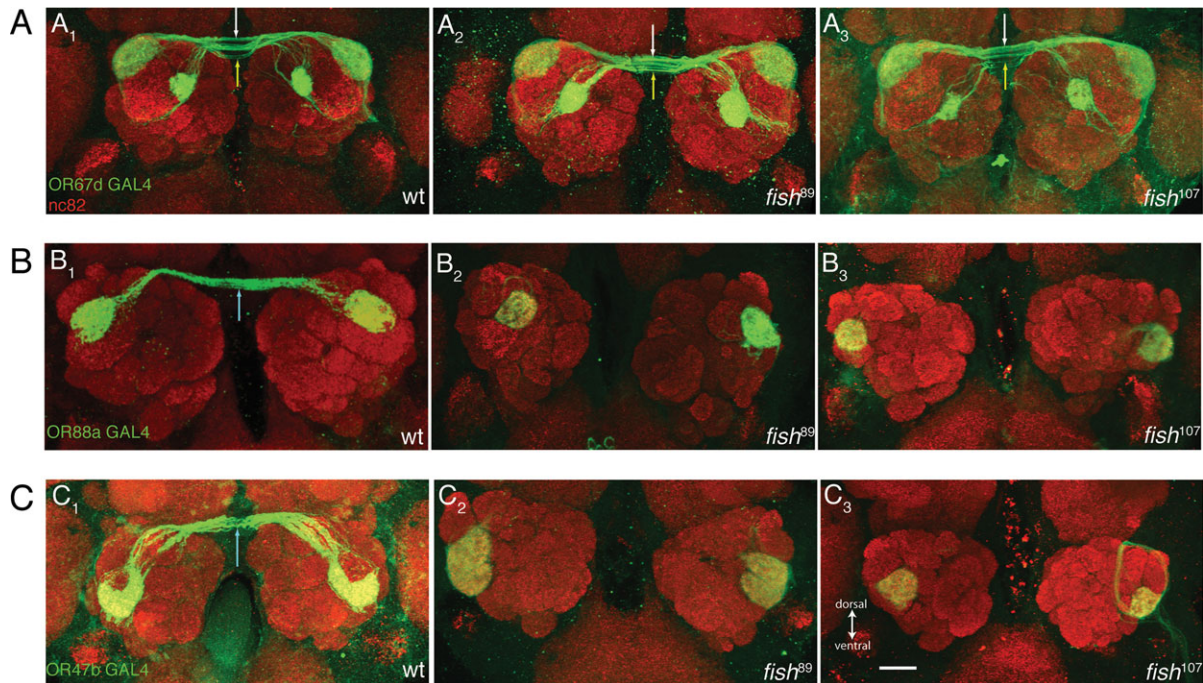
Figure 8 *Dichaete* mutant brains exhibit class-specific defects in the midline crossing of ORN axons. A: Midline crossing of *OR67d-GAL4* expressing axons is not affected in *Dichaete* mutant brains. In wild-type animals OR67d axons innervate ipsilaterally in glomerulus DA1 and cross the midline (arrows) to innervate the corresponding contralateral DA1 glomerulus (A_1). This projection pattern was not altered in D^{89} (A_2) or D^{107} (A_3) mutant brains. *OR67d-GAL4* targeted mCD8GFP expression (green) and anti-nc82 immunostaining (red) is presented. B: *OR88a-Gal4* expressing axons fail to cross the midline in $\sim$40% of *Dichaete* mutant brains. In wild-type animals OR88a axons innervate ipsilaterally in glomerulus VA1d and cross the midline (arrows) to innervate in the corresponding contralateral VA1d glomerulus (B_1). In contrast in D^{89} (B_2) and D^{107} (B_3) mutant brains OR88a axons failed to cross the midline. *OR88a-GAL4* targeted mCD8GFP expression (green) and anti-nc82 immunostaining (red) is presented. C: *OR47b-Gal4* expressing axons fail to cross the midline in *Dichaete* mutant brains. In wild-type animals OR47b axons innervate ipsilaterally in glomerulus VA1l/m and cross the midline (arrows) to innervate in the corresponding contralateral VA1l/m glomerulus (C_1). In contrast, in $\sim$40% of D^{89} (C_2) and D^{107} (C_3) mutant brains OR47b axons failed to cross the midline. *OR47b-GAL4* targeted mCD8GFP expression (green) and anti-nc82 immunostaining (red) is presented. All panels are oriented as in (C_3), the scale bar in (C_3) corresponds to 20 μm. Genotypes depicted: *OR67d-GAL4; UAS-mCD8GFP* (A_1), *OR67d-GAL4; UAS-mCD8GFP; D^{89}* (A_2), *OR67d-GAL4; UAS-mCD8GFP; D^{107}, w; OR88a-GAL4, UAS-mCD8GFP* (B_1), *w; OR88a-GAL4, UAS-mCD8GFP; D^{89}* (B_2), *w; OR88a-GAL4, UAS-mCD8GFP; D^{107}* (B_3), *w; OR47b-GAL4, UAS-mCD8GFP* (C_1), *w; OR47b-GAL4, UAS-mCD8GFP; D^{89}* (C_2), *w; OR47b-GAL4, UAS-mCD8GFP; D^{107}* (C_3). [Color figure can be viewed in the online issue, which is available at wileyonlinelibrary.com.]

meruli [Fig. 5(B)], this suggests that Dichaete may also have cell nonautonomous functions in ORN axonogenesis. However, it is possible that the OR88a and OR47b contralateral projections do remain present, but do not contain detectable GFP expression, perhaps due to alterations in GFP subcellular localization. Minimally, Dichaete functions appear to be important for the properties of specific ORN axons that cross the midline.

DISCUSSION

During embryonic and larval stages, Dichaete expression is observed in a highly dynamic and diverse pattern that includes many different cell types and tissues. Indeed, the *Dichaete* gene has pleiotropic functions in these stages and influences a wide range of developmental processes (e.g., Nambu and Nambu, 1996; Russell et al., 1996; Mukherjee et al., 2000;

Sánchez-Soriano and Russell, 2000). Similarly, Dichaete expression in the adult CNS is also complex. Within the central brain, strong Dichaete expression was detected in several prominent paired clusters of neurons. This includes the LAAL cells as well as other clusters located medially and dorsally near the optic lobes, and along the dorsal margin of the protocerebrum. The ~ 225 LAAL cells minimally consist of a heterogeneous mixture of GABAergic and cholinergic LNs, as well as ring neurons of the central complex ellipsoid body. Among the Dichaete-expressing LNs are descendants of the lateral neuroblast (lNb) that gives rise to LNs, PNs, and other neuronal types. However, Dichaete expression was not detected in any PN progeny of the INb. Strong Dichaete expression was also observed in both neurons and glia in the medulla of the adult optic lobes. Many of these Dichaete-expressing cells also express Eyeless, which has highly conserved, essential functions in eye development (reviewed in Gehring, 1996). In vertebrates, the Dichaete homolog SOX2 is important for expression of lens crystallin genes and proper differentiation of eye tissues (Muta et al., 2002; Taranova et al., 2006), and human SOX2 mutations are associated with haploinsufficient bilaterial anopthalmia (Fantes et al., 2003; Ragge et al., 2005). Furthermore, SOX2 forms a functional complex with the Eyeless homolog, Pax6 that initiates lens placode development (Kamachi et al., 2001). These data suggests that the semilethal Dichaete alleles described in this study may also be useful to examine conserved functions of Sox genes in visual system development.

While Dichaete null alleles exhibit complete embryonic lethality associated with major disruptions in segmentation and nervous system formation, Dichaete mutants were first identified based on an adult phenotype affecting wing posture (Bridges and Morgan, 1923). These dominant gain-of-function phenotypes correspond to ectopic Dichaete expression in the wing hinge region that results from inversion breakpoints within Dichaete gene regulatory regions (Russell, 2000). The semilethal D^{107}, D^{89}, and D^{175} mutations described in this study appear to be hypomorphic regulatory alleles. Thus, each excision mutant contains only internal deletion(s) within the PZ P element of P[rJ375] (Nambu and Nambu, 1996); none contain a detectable deletion of the Dichaete coding region or intron. Analysis of Dichaete mutant adult brains revealed a mosaic reduction of Dichaete protein expression levels. Both D^{89} and D^{107} exhibited strongly reduced Dichaete expression in the optic lobes and D^{89} mutants also exhibited an overall reduction of Dichaete expression in most sites within the central brain, including the

LAAL cells. In contrast, Dichaete expression in D^{107} brains is not as strongly diminished in LAAL cells, but is reduced in other brain regions. The milder disruption of Dichaete expression in D^{107} compared with D^{89} is consistent with the greater viability of this allele.

The incomplete penetrance of PN defects in Dichaete mutants could be a consequence of alterations in Dichaete expression in a specific subset of LNs essential for PN targeting: Dichaete expression may not be uniformly disrupted in every individual mutant. Alternatively, the incomplete penetrance of Dichaete mutant phenotypes might reflect a specific biochemical role for Dichaete protein where reduced levels of Dichaete function may only incompletely disrupt expression of specific Dichaete target genes.

Overall, the data suggest that the loss of internal P element sequences in the D^{89} and D^{107} alleles results in disruption of proper transcriptional regulation of the native Dichaete gene. As the original P element insertion associated with P[rJ375] enhancer trap strain does not appear to alter Dichaete gene function or expression, the internal deletions in the viable excision mutants may result in the formation of novel sequences within the P element that impact Dichaete gene transcription. These sequences could correspond to ectopic repressor elements that disrupt the actions of brain enhancer elements in the native Dichaete gene. Alternately, in all three Dichaete mutants the $5'$ end of the lacZ gene is intact; thus, it is possible an aberrant RNA transcript is generated that disrupts Dichaete gene transcription in the adult brain. While limited data is available for comparison, internal P element excisions have been shown to influence expression of the vestigial and yellow genes (Geyer et al., 1988; Hodgetts and O'Keefe, 2001).

Significantly, while viable Dichaete mutants exhibited alterations in PN dendritic and axonal processes, Dichaete expression was not detected in any mature or developing PNs, and analysis of D^{87} mutant clones indicated that loss of Dichaete function in developing GH146-GAL4 PNs did not result in detectable PN abnormalities. In addition, Dichaete was not identified in a search for PN transcription factors important for PN dendritic targeting (Komiyama and Luo, 2007). These observations suggest that Dichaete influences PN differentiation via noncell-autonomous mechanisms. In this case, what are the relevant sites of Dichaete expression for PN differentiation? Within the glomeruli, PNs interact with both ORNs and LNs. No Dichaete expression was detected in developing antennal ORNs, strongly suggesting that they are not the relevant cell type. However, prominent Dichaete expression was observed in multiple LN types present
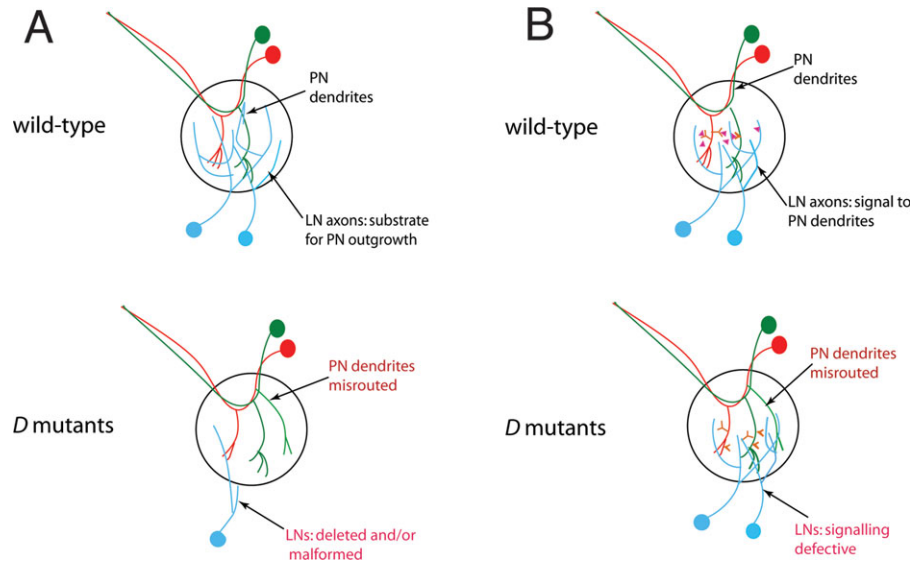
Figure 9 Two models for requirement of *Dichaete* function in LNs for PN dendritic targeting. A: The LNs could provide a physical substrate for PN dendritic outgrowth. In wild type brains PN dendrites grow out and/or extend class-specific branches on LN neurites. LN neurite innervation in the developing AL is drastically disrupted in *D* mutant brains, and PN dendrites are mistargeted as a consequence of lacking the normal substrate to grow along. B: The LNs could provide a developmental signal to PNs. In wild type brains, LN neurites would provide a diffusible or contact-mediated signal to PN dendrites to facilitate their class-specific dendritic branching. In *Dichaete* mutant brains, PN dendrites are mistargeted as a consequence of defective LN-PN signaling.

in LAAL clusters that are in close proximity to PNs. While any of these LAAL cells could interact with neighboring PNs, given their axonal projections into the AL, the Dichaete-expressing LNs are particularly attractive candidates. This suggests two potential, nonmutually exclusive models. One possibility is that a loss of specific LNs in *Dichaete* mutants might deprive PN dendrites of a physical substrate necessary to guide proper growth into and targeting within the AL [Fig. 9(A)]. However, while *Dichaete* mutant brains did exhibit slight displacement of some LN cell bodies, there did not appear to be significant alterations in LN numbers or projection patterns. LN organization was largely unaltered. Thus, it seems unlikely that LN neurites serve merely a physical substrate for PN dendrite outgrowth. A distinct possibility is that some or all LNs participate in a signaling pathway that influences PN dendritic elaboration. Interestingly, Chou et al. (2010b) recently demonstrated that Hedgehog protein secreted by AL neurons into the developing AL is required for the targeting of many ORN classes. Thus there is significant precedent to suggest that cell nonautonomous signals direct the targeting of olfactory neural processes. Given the close proximity of LN and PN processes, such a signal could be mediated via direct cell/cell contact or

over short distances [Fig. 9(B)]. Identification of specific LN and PN classes that may be involved in this signaling pathway remains to be determined. *GH146-GAL4* lPN targeting and differentiation were normal in D^{87} null mutant lNb clones where Dichaete function is lost in lNb-derived LNs. This result indicates that Dichaete function is not required in lNb-derived LNs for differentiation of *GH146-GAL4* (and therefore, *Mz19-GAL4*) lPNs. However, it remains possible that Dichaete function is required in lNb-derived LNs for the targeting and differentiation of *Mz19-GAL4* adPNs. Careful examination of the *Mz19*-GAL4 PN defects in *Dichaete* mutants appears to support of this idea. Thus, in all instances of *Dichaete* mutants where *Mz19-GAL4* PN dendrites innervated a single glomerulus, that glomerulus appeared to be DA1, normally a target of lPNs. This phenotype was frequently accompanied by a loss of *Mz19-GAL4* adPNs, supporting the notion that innervation of *Mz19-GAL4* adPN target glomeruli is selectively lost in *Dichaete* mutants. Alternatively, Dichaete function could be required in a novel subset of LNs that do not derive from the lNb.

Similarly, proper midline crossing of axons from specific ORN classes may also require noncell autonomous functions of Dichaete. Thus, the contralateral

but not ipsilateral projections of *OR88a-Gal4*, *UAS-mCD8GFP* and *OR47b-Gal4*, *UAS-mCD8GFP* expressing neurons lack GFP expression in *Dichaete* mutants, even though Dichaete is not expressed in these ORNs. This effect is cell-type specific as both the ipsilateral and contralateral projections of *ORD67d-GAL4*; *UAS-mCD8GFP* expressing neurons are unaffected in *Dichaete* mutant brains and exhibit the same GFP expression pattern as observed in a wild type background. While the basis for this ORN axon defect is uncertain and could reflect disruptions in GFP localization as opposed to ORN axon guidance, the midline crossing of ORN axons has been found to require Robo2 in the ORNs themselves and Slit in an unidentified cell type (Jhaveri et al., 2004). It is possible that Dichaete may influence Slit expression in relevant adult brain cell types similarly to its regulation of Slit expression in the embryonic CNS midline (Soriano and Russell, 1998; Ma et al., 2000). Another potential explanation for the ORN axon defects in *Dichaete* mutants is that the OR88a and OR47b axons may require guidance cues from a set of LN axons that project across the midline (Chou et al., 2010a). *Dichaete* mutants could disrupt the functions of these LNs, thereby altering midline guidance signals utilized by some ORNs. At this point there is no compelling data supporting either explanation and the unaffected midline crossing of OR67d axons in *Dichaete* mutants suggests highly specific guidance defects.

In summary, this study identifies a role for the Dichaete Sox protein in the organization of the adult *Drosophila* olfactory circuit. Dichaete expression was observed in discrete clusters of neurons within the *Drosophila* adult brain that were shown to include excitatory and inhibitory LNs as well as several central complex ring neurons. No Dichaete expression was detected in PNs or ORNs. Analysis of novel viable *Dichaete* mutant alleles revealed functions for Dichaete in the proper elaboration of dendritic and axonal processes of specific PNs. Normal differentiation of PNs thus appears to require input from distinct Dichaete-expressing cells. It is of interest to ultimately identify the nature and source of this input and characterize the Dichaete-dependent processes that contribute to olfactory circuit formation.

REFERENCES

Brazel ,CY, Limke TL, Osborne JK, Miura T, Cai J, Pevny L, Rao MS. 2005. Sox2 expression defines a heterogeneous population of neurosphere-forming cells in the adult murine brain. Aging Cell 4:197–207.

Bridges CB, Morgan TH. 1923. The third-chromosome group of mutant characters of *Drosophila melanogaster*. Pub Carnegie Inst 327:1–251.

Buescher M, Hing FS, Chia W. 2002. Formation of neuroblasts in the embryonic central nervous system of *Drosophila melanogaster* is controlled by SoxNeuro. Development 129:4193–4203.

Chew L-J, Gallo V. 2009. The yin and yang of SOX proteins: Activation and repression in development and disease. J Neurosci Res 87:3277–3287.

Chou ,Y-A, Spletter ML, Yaski E, Leong JCS, Wilson RI, Luo L. 2010a. Diversity and wiring variability of olfactory local interneurons in the *Drosophila* antennal lobe. Nat Neurosci 13:439–449.

Chou YH, Zheng X, Beachy PA, Luo L. 2010b. Patterning axon targeting of olfactory receptor neurons by coupled hedgehog signaling at two distinct steps. Cell 142:954–966.

Couto A, Alenius M, Dickson BJ. 2005. Molecular, anatomical, and functional organization of the Drosophila olfactory system. Curr Biol 15:1535–1547.

Das A, Sen S, Lichtneckert R, Okada R, Ito K, Rodrigues V, Reichert H. 2008. *Drosophila* olfactory local interneurons and projection neurons derive from a common neuroblast lineage specified by the empty spiracles gene. Neural Dev 3:33–49.

Dong C, Wilhelm D, Koopman P. 2004. Sox genes and cancer. Cytogenet Genome Res 105:442–447.

Fantes J, Ragge NK, Lynch SA, McGill NI, Collin JR, Howard-Peebles PN, Hayward C, et al. 2003. Mutations in SOX2 cause anopthalmia. Nat Genet 33:461–463.

Fishilevich E, Vosshall LB. 2005. Genetic and functional subdivision of the *Drosophila* antennal lobe. Curr Biol 15:1548–1553.

Gehring WJ. 1996. The master control gene for morphogenesis and evolution of the eye. Genes Cells 1:11–15.

Geyer PK, Richardson KL, Corces VG, Green MM. 1988. Genetic instability in *Drosophila melanogaster*: P-element mutagenesis by gene conversion. Proc Nat Acad Sci USA 85:6455–6459.

Hamasaka Y, Wegener C, Nässel DR. 2005. GABA modulates *Drosophila* circadian clock neurons via $GABA_B$ receptors and decreases in calcium. J Neurobiol 65:225–240.

Hodgetts RB, O'Keefe SL. 2001. The mutant phenotype associated with P-element alleles of the vestigial locus in *Drosophila melanogaster* may be caused by a read-through transcript initiated at the P-element promoter. Genetics 157:1665–1672.

Huang J, Zhang W, Qiao W, Hu A, Wang Z. 2010. Functional connectivity and selective odor responses of excitatory local interneurons in *Drosophila* antennal lobe. Neuron 67:1021–1033.

Ito K, Sass H, Urban J, Hofbauer A, Schneuwly S. 1997. *GAL4*-responsive UAS-tau as a tool for studying the anatomy and development of the *Drosophila* central nervous system. Cell Tissue Res 290:1–10.

Jhaveri D, Saharan S, Sen A, Rodrigues V. 2004. Positioning sensory terminals in the olfactory lobe of *Drosophila* by Robo signalling. Development 13:1903–1912.

Jefferis GS, Vyas RM, Berdnik D, Ramaekers A, Stocker RF, Tanaka NK, Ito K, et al. 2004. Developmental origin of wiring specificity in the olfactory system of *Drosophila*. Development 131:117–130.

Jefferis GS, Marin EC, Stocker RF, Luo L. 2001. Target neuron prespecification in the olfactory map of *Drosophila*. Nature 414:204–208.

Kamachi Y, Uchikawa M, Tanouchi A, Sekido R, Kondoh H. 2001. Pax6 and SOX2 form a co-DNA-binding partner complex that regulates initiation of lens development. Genes Dev 15:1272–1286.

Kiefer JC. 2007. Back to basics: SOX genes. Dev Dyn 236:2356–2366.

Komiyama T, Luo L. 2007. Intrinsic control of precise dendritic targeting by an ensemble of transcription factors. Curr Biol 17:278–285.

Komiyama T, Carlson JR, Luo L. 2004. Olfactory receptor neuron axon targeting: Intrinsic transcriptional control and hierarchical interactions. Nat Neurosci 7:819–825.

Komiyama T, Johnson WA, Luo L, Jefferis GS. 2003. From lineage to wiring specificity. POU domain transcription factors control precise connections of *Drosophila* olfactory projection neurons. Cell 112:157–167.

Krashes MJ, Keene AC, Leung B, Armstrong JD, Waddell S. 2007. Sequential use of mushroom body neuron subsets during *Drosophila* odor memory processing. Neuron 53:103–115.

Lai SL, Awasaki T, Ito K, Lee T. 2008. Clonal analysis of *Drosophila* antennal lobe neurons: Diverse neuronal architectures in the lateral neuroblast lineage. Development 135:2883–2893.

Lefebvre V, Dumitriu B, Penzo-Mendez A, Han Y, Pallavi B. 2007. Control of cell fate and differentiation by Sry-related high-mobility-group box (SOX) transcription factors. Int J Biochem Cell Biol 39:2195–2214.

Ma Y, Certel K, Gao Y, Niemitz E, Mosher J, Mukherjee A, Mutsuddi M, et al. 2000. Functional interactions between *Drosophila* bHLH/PAS, SOX, and POU transcription factors regulate CNS midline expression of the *slit* gene. J Neurosci 20:4596–4605.

Ma Y, Niemitz EL, Nambu PA, Shan X, Sackerson C, Fujioka M, Goto T, et al. 1998. Gene regulatory functions of *Drosophila* Fish-hook, a high mobility group HMG domain Sox protein. Mech Dev 73:169–182.

Mathew D, Gramates LS, Packard M, Thomas U, Bilder D, Perrimon N, Gorczyca M, et al. 2002. Recruitment of scribble to the synaptic scaffolding complex requires GUK-holder, a novel DLG binding protein. Curr Biol 12:531–539.

Muta M, Kamachi Y, Yoshimoto A, Higashi Y, Kondoh H. 2002. Distinct roles of SOX2, Pax6 and Maf transcription factors in the regulation of lens-specific delta1-crystallin enhancer. Genes Cells 7:791–805.

Mukherjee A, Shan X, Mutsuddi M, Ma Y, Nambu JR. 2000. The *Drosophila* sox gene, *fish-hook*, is required for postembryonic development. Dev Biol 217:91–106.

Nambu PA, Nambu JR. 1996. The *Drosophila fish-hook* gene encodes a HMG domain protein essential for segmentation and CNS development. Development 122:3467–3475.

Ng M, Roorda RD, Lima SQ, Zemelman BV, Morcillo P, Miesenbock G. 2002. Transmission of olfactory information between three populations of neurons in the antennal lobe of the fly. Neuron 36:463–474.

Olsen SR, Bhandawat V, Wilson RI. 2007. Excitatory interactions between olfactory processing channels in the *Drosophila* antennal lobe. Neuron 54:89–103.

Overton PM, Meadows LA, Urban J, Russell S. 2002. Evidence for differential and redundant function of the SOX genes *Dichaete* and *SOXN* during CNS development in *Drosophila*. Development 129:4219–4228.

Ragge NK, Lorenz B, Schneider A, Bushby K, de Sanctis L, de Sanctis U, Salt A, et al. 2005. SOX2 anopthalmia syndrome. Am J Med Genet A 135:1–7.

Renn SC, Armstrong JD, Yang M, Wang Z, An X, Kaiser K, Taghert PH. 1999. Genetic analysis of the *Drosophila* ellipsoid body neuropil: Organization and development of the central complex. J Neurobiol 41:189:207.

Rodrigues V, Hummel T. 2008. Development of the *Drosophila* olfactory system. In: Technau GM, editor. Brain Development in *Drosophila melanogaster*. Landes Biosciences and Springer Science. pp 82–101.

Russell S. 2000. The *Drosophila* dominant wing mutation *Dichaete* results from ectopic expression of a SOX-domain gene. Mol Gen Genet 263:690–701.

Russell SR, Sanchez-Soriano N, Wright CR, Ashburner M. 1996. The *Dichaete* gene of *Drosophila melanogaster* encodes a SOX-domain protein required for embryonic segmentation. Development 122:3669–3676.

Salvaterra PM, Kitamoto T. 2001. *Drosophila* cholinergic neurons and processes visualized with-*GAL4*/UAS-GFP. Brain Res Gene Expr Patt 1:73–82.

Sánchez-Soriano N, Russell S. 2000. Regulatory mutations of the *Drosophila* SOX gene *Dichaete* reveal new functions in embryonic brain and hindgut development. Dev Biol 220:307–321.

Shang Y, Claridge-Chang A, Sjulson L, Pypaert M, Miesenbock G. 2007. Excitatory local circuits and their implications for olfactory processing in the fly antennal lobe. Cell 128:601–12.

Soriano NS, Russell S. 1998. The Drosophila SOX-domain protein Dichaete is required for the development of the central nervous system midline. Development 125:3989–3896.

Stocker RF, Heimbeck G, Gendre N, de Belle JS. 1997. Neuroblast ablation in *Drosophila* P[GAL4] lines reveals origins of olfactory interneurons. J Neurobiol 32:443–456.

Sweeney LB, Couto A, Chou YH, Berdnik D, Dickson BJ, Luo L, Komiyama T. 2007. Temporal target restriction of olfactory receptor neurons by Semaphorin1a/PlexinA-mediated axon-axon interactions. Neuron 53:185–200.

Taranova OV, Magness ST, Fagan BM, Wu Y, Surzenko N, Hutton SR, Pevny LH. 2006. SOX2 is a dose-dependent regulator of retinal neural progenitor competence. Genes Dev 20:1187–1202.

Venken KJ, Carlson JW, Schulze KL, Pan H, He Y, Spokony R, Wan KH, et al. 2009. Versatile P[acman] BAC libraries for transgenesis studies in *Drosophila melanogaster*. Nat Methods 6:431–434.

Vosshall LB, Stocker RF. 2007. Molecular architecture of smell and taste in *Drosophila*. Annu Rev Neurosci 30:505–33.

Vosshall LB, Wong AM, Axel R. 2000. An olfactory sensory map in the fly brain. Cell 102:147–159.

Wang TW, Stromberg GP, Whitney JT, Brower NW, Klymkowsky MW, Parent JM. 2006. Sox3 expression identifies neural progenitors in persistent neonatal and adult mouse forebrain germinative zones. J Comp Neurol 497:88–100.

Wilson RI, Laurent G. 2005. Role of GABAergic inhibition in shaping odor-evoked spatiotemporal patterns in the *Drosophila* antennal lobe. J Neurosci 25:9069–9079.

Wilson RI, Turner GC, Laurent G. 2004. Transformation of olfactory representations in the *Drosophila* antennal lobe. Science 303:366–370.

Wu JS, Luo L. 2006a. A protocol for mosaic analysis with a repressible cell marker (MARCM) in *Drosophila*. Nat Protoc 1:2583–2589.

Wu JS, Luo L. 2006b. A protocol for dissecting *Drosophila melanogaster* brains for live imaging or immunostaining. Nat Protoc 1:2110–2115.

Yaksi E, Wilson RI. 2010. Electrical coupling between olfactory glomeruli. Neuron 67:1034–1047.

Yao KM, White K. 1994. Neural specificity of Elav expression: defining a *Drosophila* promoter for directing expression to the nervous system. J Neurochem 63:41–51.

Zhao G, Boekhoff-Falk G, Wilson BA, Skeath JB. 2007. Linking pattern formation to cell-type specification: Dichaete and Ind directly repress *achaete* gene expression in the *Drosophila* CNS. Proc Natl Acad Sci USA 104:3847–3852.

Zhao G, Skeath JB. 2002. The SOX-domain containing gene *Dichaete/fish-hook* acts in concert with *vnd* and *ind* to regulate cell fate in the *Drosophila* neuroectoderm. Development 129:1165–1174.

Zhu H, Luo L. 2004. Diverse functions of N-cadherin in dendritic and axonal terminal arborization of olfactory projection neurons. Neuron 42:63–75.